

Improving On-Demand Single Photon Source Coherence and Indistinguishability Through a Time-Delayed Coherent Feedback

Gavin Crowder,^{1, 2, 3, *} Lora Ramunno,^{1, 2} and Stephen Hughes³

¹*Department of Physics, University of Ottawa, Ottawa, Ontario, Canada, K1N 6N5*

²*Nexus for Quantum Technologies Institute, University of Ottawa, Ottawa, Ontario, Canada, K1N 6N5*

³*Department of Physics, Queen's University, Kingston, Ontario, Canada, K7L 3N6*

Single photon sources (SPSs) are an essential resource for many quantum information technologies. We demonstrate how the inclusion of time-delayed coherent feedback in a scalable waveguide system, can significantly improve the two key SPS figures of merit: coherence and indistinguishability. Our feedback protocol is simulated using a quantum trajectory discretized waveguide model which can be used to directly model Hanbury Brown and Twiss (HBT) and Hong-Ou-Mandel (HOM) interferometers. With the proper choice of the round trip phase, the non-Markovian dynamics from the time-delayed feedback improves the indistinguishability of the SPS by up to 57%. We also show how this mechanism suppresses the detrimental effects of off-chip decay and pure dephasing.

The reliable generation of single photons is important for the implementation of quantum information systems such as quantum cryptography and quantum computing [1]. Semiconductor quantum dots are an excellent source for generating quantum light in the form of single photons or photon pairs [2–13]. In particular, it has been shown that upon excitation by an appropriate laser pulse, preparing the quantum dot in the excited state, the dot can emit a single photon into a desired output mode, e.g., a cavity or waveguide. This generation process is termed a “on-demand” due to the production of a photon number state after each single laser pulse [14].

The key figures of merit for on-demand single photon sources (SPSs) are the brightness, η (the average number of photons per laser pulse), the second order coherence, $g^{(2)}(0)$ (related to the single photon purity), and the indistinguishability, \mathcal{I} (a measure of the coherence of the emitted photon state) [8, 15]. Significant research efforts have been developed to improve the efficiency, purity, and coherence of SPS generation. State of the art systems have achieved $g^{(2)}(0) = 0.012$ and an indistinguishability of $\mathcal{I} = 0.962$ [9], though often these numbers are after filtering. Unwanted photon pair generation, out of plane emission, and dephasing events (such as through phonon absorption/emission [16, 17]) are all key challenges to overcome for continued improvement of these SPSs.

Feedback, where the output from a system is used as a stabilizing or control mechanism, has been well used across various platforms [18–28]. This is most often implemented through measurement-based feedback, where the output is measured to inform an external control which acts on the system [24–26, 29–33]. However, this approach is problematic for quantum information systems that rely on maintaining system coherence. Instead, feedback can be included at the system level and act back on the system itself to avoid measurement: *coherent feedback*. Recently, coherent feedback in waveguide quantum electrodynamic systems was shown to significantly alter the photon output statistics with continuous-wave pump-

ing [18–23, 34–55]. Coherent delay loops have been used in previous experiments for generating quantum states of light such as cluster states [56, 57] or graph states [58], by manipulating the output field of a SPS.

Here, we show how coherent feedback can be used in the pulsed laser regime to improve the figures of merit for a practical SPS. Accurate simulation of coherent feedback is a difficult challenge in quantum circuits, since it introduces a non-Markovian dynamic. To calculate $g^{(2)}(0)$ and \mathcal{I} requires knowledge of the two-time correlation functions, which typically use the quantum regression theorem (QRT) (although other specialized approaches have been developed which avoid the QRT, but they have their own practical limits [59, 60]). The QRT relies on a Markov approximation which fails in the presence of coherent feedback and other specialized techniques must be used [61–63]. To avoid the non-Markovian dynamic, collisional models can be used which include the waveguide at the system level, rather than treating it as a reservoir. We will use and extend a recently developed quantum trajectory discretized waveguide (QTDW) model [53, 55] that combines a collisional model for the feedback section of the waveguide with the quantum trajectory formalism [64, 65]. Simulating individual realizations of the system gives insights into the underlying stochastic system dynamics and can be averaged to obtain the ensemble dynamics. Our model can also incorporate additional dephasing needed for simulating realistic quantum dots, a limitation of matrix product states, the other main technique for simulating feedback dynamics. Moreover, the QTDW model scales linearly with the number of photon states and is parallelizable.

In this Letter, we connect the QTDW model to photon correlation experiments, to compute $g^{(2)}(0)$ and \mathcal{I} for waveguide quantum electrodynamic systems with coherent feedback, yielding direct simulations of Hanbury Brown and Twiss (HBT) or Hong-Ou-Mandel (HOM) interferometers. We summarize the key features of the QTDW model and outline its extension to simulate the

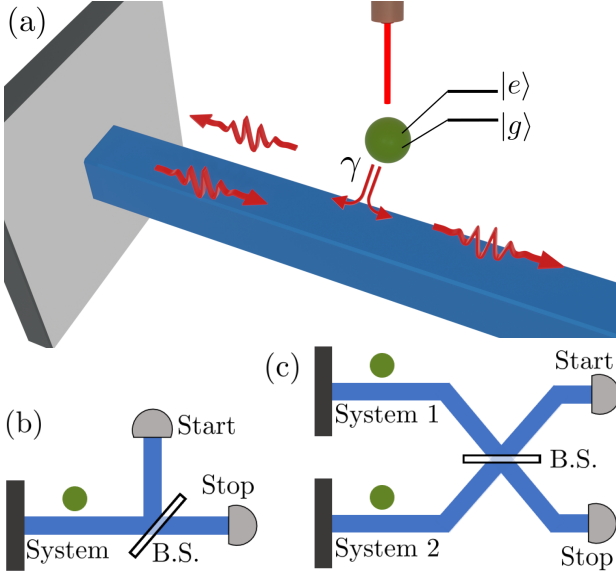


FIG. 1. Schematics of (a) the driven TLS setup with a coupled coherent feedback loop, (b) the HBT interferometer, and (c) the HOM interferometer; ‘B.S.’ represents a beam splitter.

HBT and HOM measurements. We then show how a coherent feedback can significantly improve the η , $g^{(2)}(0)$, and \mathcal{I} figures of merit for a quantum dot SPS by up to 57%, and explain this improvement in the context of the feedback dynamics.

The system of interest, as shown in Fig. 1(a), is a single two-level system (TLS) coupled to a *truncated* waveguide which acts as a feedback loop, returning the output from the TLS to itself. An input laser pulse excites the TLS for SPS emission. The total Hamiltonian in natural units ($\hbar = 1$) for the system, waveguide, and pump (in the interaction picture of the laser and with a rotating wave approximation) is $H = H_W + H_{\text{TLS}} + H_I + H_{\text{pump}}$. The TLS Hamiltonian is $H_{\text{TLS}} = \delta\sigma^+\sigma^-$ where σ^+ (σ^-) is the Pauli raising (lowering) operator and $\delta = \omega_0 - \omega_L$ is the detuning between the TLS, with frequency ω_0 , and the laser, with frequency ω_L . The pump Hamiltonian is $H_{\text{pump}} = \Omega(t)/2(\sigma^+ + \sigma^-)$ with the laser pulse shape given by $\Omega(t)$ which drives the quantum dot with a field orthogonal to the waveguide mode polarization [66–68].

In the continuous frequency domain, and in the same interaction picture, the raising (lowering) operator for the photon modes in the waveguide are $b^\dagger(\omega)$ ($b(\omega)$) with Hamiltonian $H_W = \int_{-\infty}^{\infty} d\omega (\omega - \omega_L) b^\dagger(\omega) b(\omega)$, with $[b(\omega), b^\dagger(\omega')] = \delta(\omega - \omega')$. The interaction between the waveguide and TLS, with total radiative rate γ (and symmetric left and right coupling), is described by the Hamiltonian $H_I = \int_{-\infty}^{\infty} d\omega [(\sqrt{\frac{\gamma}{4\pi}}\sigma^+ b(\omega) + \sqrt{\frac{\gamma}{4\pi}}e^{i(\phi_M + \omega\tau)}\sigma^+ b(\omega)) + \text{H.c.}]$, which incorporates the influence of the feedback loop, including the round trip delay time, τ , and a mirror phase change, ϕ_M .

To model the feedback loop, we use a QTDW tech-

nique [53, 55], where the field operators, $b(\omega)$, for the waveguide section of interest ($-L < x < 0$) are transformed into the discrete time domain with operators B_n with commutation relation $[B_n, B_{n'}^\dagger] = \delta_{n,n'}$. These operators describe a unidirectional slice of the waveguide field which travels around the feedback loop, interacting twice with the TLS, located at the beginning and end of the loop. Additional details on these time domain operators are given in the Supplementary Material [69]. In this transformation, H_{TLS} and H_{pump} are unchanged and the interaction Hamiltonian becomes

$$H_I = \left(\sqrt{\frac{\gamma}{2\Delta t}}\sigma^+ B_{N-1} + e^{i\phi} \sqrt{\frac{\gamma}{2\Delta t}}\sigma^+ B_0 \right) + \text{H.c.}, \quad (1)$$

where $\phi = \phi_M + \omega_0\tau$ is the round trip phase change and $\Delta t = \tau/N$ is the time discretization of the feedback loop; now the TLS interacts with the incoming $(N-1)^{\text{th}}$ bin (B_{N-1}) and the outgoing zeroth bin (B_0) which picks up the phase change ϕ . The key advantage of this approach appears in the evolution of the B_n operators under the waveguide Hamiltonian, which is $U_W^\dagger(\Delta t)B_nU_W(\Delta t) = e^{-i\delta\Delta t}B_{n-1}$, where $U_W(\Delta t) = e^{-iH_W\Delta t}$. This evolution acts to *pass* the waveguide field forward one bin each time step, where we assume linear dispersion.

A limitation of this approach is that the total number of waveguide photons at any instant must be truncated. Typically, this is chosen to be two to capture the interference between multiple photons in the feedback loop and is a good approximation for most waveguide QED systems [53]. For our system, where the ideal generation is a single photon per pulse, this truncation has no affect on the results. The waveguide field outside of the loop, i.e., for $x > 0$, is modeled through the incoming and outgoing feedback loop bins, and the incoming bins are vacuum fields. During the quantum trajectory step, we take a simulated measurement of the outgoing bin (B_0) and project the full ket vector accordingly. After projection, there is no information in the outgoing bin and it can be dropped to retain a tractable Hilbert space (absorbing boundary condition). This is a stochastic process, but an average over many individual trajectories yields the ensemble average behavior of the system.

Importantly (and a major advantage over matrix product states) we also include two important dissipation channels in our model of the TLS: (i) off chip decay from the TLS, $C_0 = \sqrt{\gamma_0}\sigma^-$, with rate γ_0 , and (ii) pure dephasing in the TLS, $C_1 = \sqrt{\gamma'}\sigma^+\sigma^-$, with rate γ' . These are included as quantum jump operators following standard quantum trajectory theory [64, 65].

Conventionally, the brightness, η , is calculated as the total field emitted from the qubit into the waveguide from a single laser pulse. In the ensemble average picture this is calculated as $\eta = \int_0^\infty dt' \gamma \langle \sigma^+(t')\sigma^-(t') \rangle$. In the quantum trajectory picture, the above expression can also be calculated using the average expectation of $\langle \sigma^+\sigma^- \rangle$ across all trajectories. Equivalently since each trajectory

contains a detection record of emitted photons from the waveguide, η can be calculated by taking the average number of photons emitted in a trajectory.

Using the QTDW model, we take advantage of the natural link between the individual trajectories and experiments to calculate $g^{(2)}(0)$ and \mathcal{I} through simulated HBT and HOM interferometers. While our technique can tractably calculate the two-time correlation functions, the HBT and HOM approaches are more intuitive and numerically much faster. In the HBT interferometer [70], see Fig. 1(b), the output field is sent to a 50:50 beam-splitter and entangled with the vacuum field. The two new fields are then measured by two detectors, a *start* detector and a *stop* detector, with operators $B_{\text{start}}^{\text{HBT}} = B_0/\sqrt{2}$ and $B_{\text{stop}}^{\text{HBT}} = B_0/\sqrt{2}$ (with vacuum contributions not included as they do not play a role in the measurements). The detection times between the two detectors are correlated by taking the difference between the detection time on the *start* detector and all *stop* detection events, yielding a histogram of time-correlated detection records, $h_{\text{HBT}}(t')$. The system is driven by consecutive pulses to build up a sufficient detection record, each separated by a delay time, T , long enough for the system to completely relax into the ground state before sending in the next pulse.

To simulate the HBT detection, we run each trajectory independently with a single pulse to drive the system and then allowing it to relax for a total run time of T . Next, we place these trajectories in sequential order so that each pulse is separated by T and treat it as one long single quantum trajectory. Since the beam-splitter equally splits the output field, to get the time-correlated detection records we stochastically assign each output jump event in the trajectory to either the start or stop detector and then correlate the two detection records to build the histogram, $h_{\text{HBT}}(t')$, where t' is the time difference between start and stop events. Assuming no correlations between pulses, when T is chosen sufficiently large, then

$$g^{(2)}(0) = \frac{A_{\text{HBT}}(0)}{A_{\text{HBT}}(T)} \left(1 \pm \sqrt{\frac{1}{A_{\text{HBT}}(0)} + \frac{1}{A_{\text{HBT}}(T)}} \right), \quad (2)$$

with $A_{\text{HBT}}(0)$ the area of the peak centered at 0 and $A_{\text{HBT}}(T)$ the area of the next peak, centered at T [15]. The central peak, $A_{\text{HBT}}(0)$, represents the number of pairs of photons being emitted from the system and this is normalized by $A_{\text{HBT}}(T)$, the photon count rate. Since each peak area is calculated as a count of events they carry an uncertainty of \sqrt{N} where N is the number of events. In these results a sufficiently large number of trajectories is carried out to approach an accurate average.

In the HOM simulation [71], see Fig. 1(c), we take the interference between the output of two independent copies ('1' or '2') of our system incident on a 50:50 beam splitter (which can easily be extended to an unequal beam splitter). The output bin operator from sys-

tem 1 (2) is $B_0^{(1)}$ ($B_0^{(2)}$). These are entangled on the beam splitter and sent on to the *start* and *stop* detectors, now with operators $B_{\text{start}}^{\text{HOM}} = (B_0^{(1)} + B_0^{(2)})/\sqrt{2}$ and $B_{\text{stop}}^{\text{HOM}} = (B_0^{(1)} - B_0^{(2)})/\sqrt{2}$. We again drive both copies using consecutive pulses with delay time, T , and time-correlate the detection records of the two detectors. Similar to the HBT interferometer, the correlated detection record can be used to yield a histogram, $h_{\text{HOM}}(t')$.

This HOM setup is more difficult to simulate with the quantum trajectory technique compared to the HBT interferometer, as the detection records are no longer accessible through our jump record of B_0 . Instead we entangle two copies of our system using a tensor product, so that the total Hamiltonian is $H_{\text{HOM}} = H^{(1)} \otimes H^{(2)}$, since the two systems are completely independent to begin with. Then, rather than taking our output operators to be $B_0^{(1)}$ and $B_0^{(2)}$, we use the entangled fields after the beam-splitter $B_{\text{start}}^{\text{HOM}}$ and $B_{\text{stop}}^{\text{HOM}}$. Next, when we detect a photon in the *start* (*stop*) detector, we apply the operator $B_{\text{start}}^{\text{HOM}}$ ($B_{\text{stop}}^{\text{HOM}}$) to the combined system. Detection times are recorded to build up detection records for the two detectors which we can time-correlate. Similarly to the HBT interferometer, from $h_{\text{HOM}}(t')$ one can calculate,

$$g_{\text{HOM}}^{(2)}(0) = \frac{A_{\text{HOM}}(0)}{A_{\text{HOM}}(T)} \left(1 \pm \sqrt{\frac{1}{A_{\text{HOM}}(0)} + \frac{1}{A_{\text{HOM}}(T)}} \right), \quad (3)$$

which is related to the indistinguishability through [8, 15]

$$\mathcal{I} = 1 - g_{\text{HOM}}^{(2)}(0). \quad (4)$$

Without feedback, i.e., for a TLS coupled to an open waveguide [6, 8, 67, 72], to generate a SPS we pump the system with a π -pulse to excite the TLS and decay back to the ground state, emitting a single photon. Note that we correct for the bi-directional output in the results without feedback so both output fields are accounted for. In the limit of an infinitely short pulse width, and neglecting other decoherence effects such as phonon interactions [8], this TLS is a perfect SPS with $g^{(2)}(0) = 0$ and $\mathcal{I} = 1$. The perfection of these sources fail when a finite pulse width is taken to account (as this introduces a chance of two photon emission) and sources of detuning and off-chip decay are included (which spoils coherence) [73]. The TLS is driven by a Gaussian π -pulse, defined by $\Omega(t) = (\pi/\sigma\sqrt{2\pi}) \exp[-t^2/2\sigma^2]$, where $\sigma = t_p/2\sqrt{2\ln 2}$ and t_p is the FWHM pulse width.

To include feedback, the delay time, τ , and the phase change, ϕ , must be strategically chosen to yield the best results. We found this occurs when the non-Markovian feedback returns just after the pulse has finished driving the system, $\tau = 3t_p$, and with a constructive interference, $\phi = 0$. The choice of delay time is discussed in the Supplementary Material [69]. This works to limit both

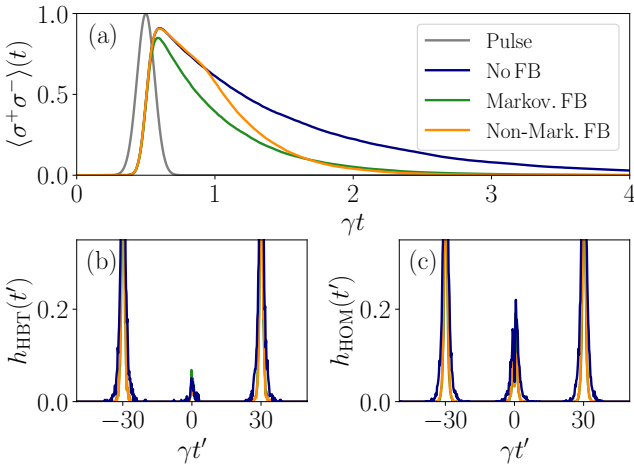


FIG. 2. (a) The TLS population dynamics without feedback, with Markovian feedback, and with non-Markovian feedback for a pulse with width $\gamma t_p = 0.15$. For this pulse width, the delay time used is $\gamma\tau = 3\gamma t_p = 0.45$ so the non-Markovian feedback returns after the pulse. No additional loss channels are included. In (b) and (c), the center peaks of the resulting HBT and HOM histograms for this feedback and pulse setup respectively, with pure dephasing (using $\gamma' = \gamma$).

of the primary drawbacks to a perfect SPS: pair emission and additional loss channels. Pair emission occurs when the TLS emits a photon during the pulse and is re-excited, emitting a second photon. Thus, to minimize pair emission, a weak decay rate from the system during the pulse is best. However, in realistic systems, the TLS is limited by off-chip decay and pure dephasing. To minimize these, the TLS should decay as quickly as possible. Hence, a time-delayed coherent feedback works optimally to improve the SPS by not increasing the decay rate until after the pulse has finished interacting with the TLS. In Fig. 2(a), the TLS population dynamics ($\langle \sigma^+ \sigma^- \rangle(t)$) show how the delay in the non-Markovian feedback begins after the pulse has fully passed and the TLS decays much faster than the dynamics without feedback. This also yields the proper choice of T to ensure the TLS has completely decayed into the ground state, which is taken to be $\gamma T = 20$ (well after the decay in Fig. 2(a)) in the HBT and HOM simulations. For the pulse widths in these results, $0.05 \leq \gamma t_p \leq 0.25$, this gives a range of delay times between $0.15 \leq \gamma\tau \leq 0.75$. This range is equivalent to a delay line with length 4.5 mm to 22.5 mm in a photonic crystal waveguide with $n_g = 10$ for a quantum dot system such as in [74] with a decay rate of $\gamma \approx 1 \text{ ns}^{-1}$.

Figure 3 shows improvements in the brightness, second order coherence, and indistinguishability when non-Markovian coherent feedback is included. We display results with and without feedback as a function of changing pulse width, off chip decay rate, and pure dephasing rate. In Figs. 3(a), (e), and (i) no additional loss channels are

included so the only factor resulting in an imperfect SPS is pair emission. As shown in Fig. 2(a), the dynamics without and with a non-Markovian feedback have the same decay rate while the pulse drives the TLS so they undergo the same rate of pair emission. Thus, the SPS acts equally well with and without feedback.

When a realistic SPS is considered, i.e., with additional loss channels, the improvement with feedback is clearly seen. In Figs. 3(b), (f), and (j) we vary the pulse width but now have off-chip decay with rate $\gamma_0 = 0.1\gamma$ and pure dephasing with rate $\gamma' = 0.5\gamma$. The brightness is primarily affected by the off-chip loss as it introduces a new channel for the TLS to decay into, rather than the waveguide; thus, for some pulses, no corresponding photon detection is found. Across all pulse widths we find an average relative improvement of 39% in the brightness. The second order coherence is primarily affected by the pair emission from the system and so there is minimal relative improvement of 3.5% with feedback as the rates of pair emission are identical. Pure dephasing events spoil the coherence of the emitted photons and so have the largest affect on the indistinguishability. With feedback, the SPS has an average relative improvement of 35% in the indistinguishability.

A Markovian feedback, $\tau \rightarrow 0^+$, will also increase the spontaneous emission rate at all times when $\phi = 0$ [18] as shown in Fig. 2(a). This will also improve the SPS performance in the presence of off-chip decay and pure dephasing, in an identical way as including a Purcell factor of 2. Crucially though, this also increases the pair emission rate which detrimentally affects the SPS. See the Supplementary Material [69] for a comparison between the improvements with Markovian and non-Markovian feedback where Markovian feedback produces a worse coherence and indistinguishability in all cases. A similar effect in a coupled cavity-TLS setup has been shown in [17] where a non-Markovian Purcell factor can arise in the bad cavity regime with pulsed excitation.

We also compare η , $g^{(2)}(0)$ and \mathcal{I} with and without feedback as a function of the off-chip decay rate in Figs. 3(c), (g), and (k), and as a function of the pure dephasing rate in Figs. 3(d), (h), and (l), with a fixed pulse width of $\gamma t_p = 0.15$. We find that for off-chip decay (Figs. 3(c), (g), and (k)), feedback does an excellent job of suppressing the effects of the additional output channel, decreasing the impact on brightness by 26%, coherence by 39% and on indistinguishability by 57%. For the pure dephasing rate (Figs. 3(d), (h), and (l)), η and $g^{(2)}(0)$ are minimally affected by the increase in pure dephasing events so there is little difference between the results with and without feedback. Pure dephasing has its greatest affect on the indistinguishability, and feedback does a good job of reducing its impact, suppressing its effects by 44%. Figure 2(c) shows an example HOM histogram when $\gamma' = \gamma$ highlighting the decreased area of the central peak in the case with non-Markovian feedback

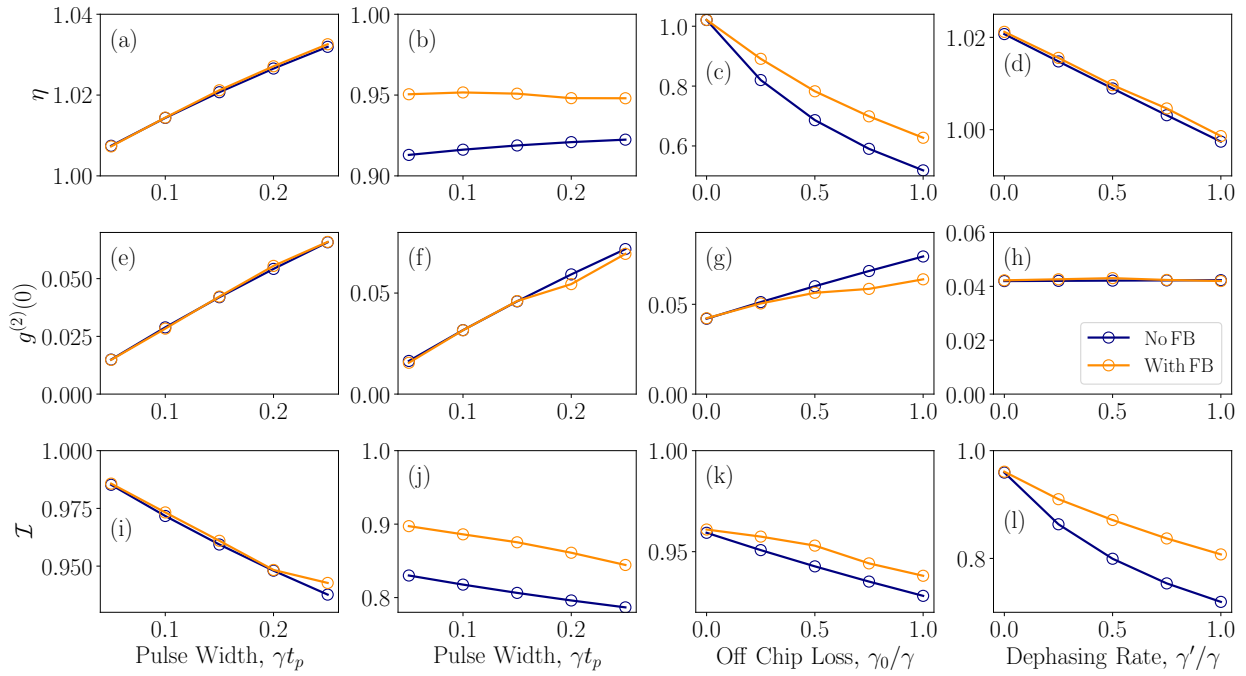


FIG. 3. (a)-(d) The brightness, (e)-(h) the second order coherence, and (i)-(l) the indistinguishability of the output single photons. The width of the incoming pulse is varied without additional dissipation channels C_0 and C_1 in (a), (e), and (i), while these channels are included ($\gamma_0 = 0.1\gamma$ and $\gamma' = 0.5\gamma$) in (b), (f), and (j). The pulse width is then set at $\gamma t_p = 0.15$ and the off chip decay rate is varied in (c), (g), and (k) with $\gamma' = 0$, while the pure dephasing rate is varied in (d), (h), and (l) with $\gamma_0 = 0$. Each data point with feedback is an average of 100,000 trajectories for η and $g^{(2)}(0)$, and 20,000 trajectories for \mathcal{I} .

leading to the improvement in indistinguishability.

In summary, we have exploited a QTDW model to calculate the $g^{(2)}(0)$ and \mathcal{I} figures of merit for a SPS by directly simulating an HBT or HOM interferometer. This approach allows one to bypass the quantum regression theorem in order to simulate the non-Markovian dynamics that arise when coherent feedback is included in a waveguide quantum electrodynamic system. Using this technique, we have shown that direct inclusion of a time-delayed coherent feedback can improve the brightness, coherence, and indistinguishability of a SPS, even when pure dephasing is a significant source of decoherence in the system. This work harnesses a single characteristic of feedback, namely its ability to enhance spontaneous emission, in order to achieve these improvements. In future work, other aspects of feedback such as excitation trapping and additional nonlinear behavior are also expected to be useful for photon pair emission and other quantum information system objectives.

This work was supported by the Natural Sciences and Engineering Research Council of Canada (NSERC), the National Research Council of Canada (NRC) through the Small Teams Ideation Program QPIC, Queen's University, and the University of Ottawa. We thank Dan Dalacu and Robin Williams for support and useful discussions.

* gcrow088@uottawa.ca

- [1] A. Kiraz, M. Atatüre, and A. Imamoğlu, Quantum-dot single-photon sources: Prospects for applications in linear optics quantum-information processing, *Physical Review A* **69**, 032305 (2004).
- [2] C. Santori, D. Fattal, J. Vučković, G. S. Solomon, E. Waks, and Y. Yamamoto, Submicrosecond correlations in photoluminescence from InAs quantum dots, *Physical Review B* **69**, 205324 (2004).
- [3] K. Takemoto, Y. Sakuma, S. Hirose, T. Usuki, N. Yokoyama, T. Miyazawa, M. Takatsu, and Y. Arakawa, Non-classical Photon Emission from a Single InAs/InP Quantum Dot in the 1.3-μm Optical-Fiber Band, *Japanese Journal of Applied Physics* **43**, L993 (2004).
- [4] G. Cui and M. G. Raymer, Emission spectra and quantum efficiency of single-photon sources in the cavity-QED strong-coupling regime, *Physical Review A* **73**, 053807 (2006).
- [5] Y.-M. He, Y. He, Y.-J. Wei, D. Wu, M. Atatüre, C. Schneider, S. Höfling, M. Kamp, C.-Y. Lu, and J.-W. Pan, On-demand semiconductor single-photon source with near-unity indistinguishability, *Nature Nanotechnology* **8**, 213 (2013).
- [6] S. Kalliakos, Y. Brody, A. Schwagmann, A. J. Bennett, M. B. Ward, D. J. P. Ellis, J. Skiba-Szymanska, I. Farrer, J. P. Griffiths, G. A. C. Jones, D. A. Ritchie, and A. J. Shields, In-plane emission of indistinguishable photons generated by an integrated quantum emitter, *Applied*

Physics Letters **104**, 221109 (2014), publisher: American Institute of Physics.

[7] M. Paul, J. Kettler, K. Zeuner, C. Clausen, M. Jetter, and P. Michler, Metal-organic vapor-phase epitaxy-grown ultra-low density InGaAs/GaAs quantum dots exhibiting cascaded single-photon emission at 1.3 μ m, *Applied Physics Letters* **106**, 122105 (2015).

[8] S. Hughes, S. Franke, C. Gustin, M. Kamandar Dezfouli, A. Knorr, and M. Richter, Theory and Limits of On-Demand Single-Photon Sources Using Plasmonic Resonators: A Quantized Quasinormal Mode Approach, *ACS Photonics* **6**, 2168 (2019).

[9] Y.-M. He, H. Wang, C. Wang, M.-C. Chen, X. Ding, J. Qin, Z.-C. Duan, S. Chen, J.-P. Li, R.-Z. Liu, C. Schneider, M. Atatüre, S. Höfling, C.-Y. Lu, and J.-W. Pan, Coherently driving a single quantum two-level system with dichromatic laser pulses, *Nature Physics* **15**, 941 (2019).

[10] P. Laferrière, E. Yeung, I. Miron, D. B. Northeast, S. Hafouz, J. Lapointe, M. Korkusinski, P. J. Poole, R. L. Williams, and D. Dalacu, Unity yield of deterministically positioned quantum dot single photon sources, *Scientific Reports* **12**, 6376 (2022).

[11] M. H. Appel, A. Tiranov, S. Pabst, M. L. Chan, C. Starup, Y. Wang, L. Midolo, K. Tiurev, S. Scholz, A. D. Wieck, A. Ludwig, A. S. Sørensen, and P. Lodahl, Entangling a Hole Spin with a Time-Bin Photon: A Waveguide Approach for Quantum Dot Sources of Multiphoton Entanglement, *Physical Review Letters* **128**, 233602 (2022).

[12] L. Ginés, M. Moczała-Dusanowska, D. Dlaka, R. Hošák, J. R. Gonzales-Ureta, J. Lee, M. Ježek, E. Harbord, R. Oulton, S. Höfling, A. B. Young, C. Schneider, and A. Predojević, High Extraction Efficiency Source of Photon Pairs Based on a Quantum Dot Embedded in a Broadband Micropillar Cavity, *Physical Review Letters* **129**, 033601 (2022).

[13] B. Da Lio, C. Faurby, X. Zhou, M. L. Chan, R. Uppu, H. Thyrrstrup, S. Scholz, A. D. Wieck, A. Ludwig, P. Lodahl, and L. Midolo, A Pure and Indistinguishable Single-Photon Source at Telecommunication Wavelength, *Advanced Quantum Technologies* **5**, 2200006 (2022).

[14] T. K. Bracht, M. Cosacchi, T. Seidelmann, M. Cygorek, A. Vagov, V. M. Axt, T. Heindel, and D. E. Reiter, Swing-Up of Quantum Emitter Population Using Detuned Pulses, *PRX Quantum* **2**, 040354 (2021).

[15] K. A. Fischer, K. Müller, K. G. Lagoudakis, and J. Vučković, Dynamical modeling of pulsed two-photon interference, *New Journal of Physics* **18**, 113053 (2016).

[16] J. Iles-Smith, D. P. S. McCutcheon, A. Nazir, and J. Mørk, Phonon scattering inhibits simultaneous near-unity efficiency and indistinguishability in semiconductor single-photon sources, *Nature Photonics* **11**, 521 (2017).

[17] C. Gustin and S. Hughes, Pulsed excitation dynamics in quantum-dot-cavity systems: Limits to optimizing the fidelity of on-demand single-photon sources, *Phys. Rev. B* **98**, 045309 (2018).

[18] U. Dorner and P. Zoller, Laser-driven atoms in half-cavities, *Physical Review A* **66**, 023816 (2002).

[19] T. Tufarelli, F. Ciccarello, and M. S. Kim, Dynamics of spontaneous emission in a single-end photonic waveguide, *Physical Review A* **87**, 013820 (2013).

[20] A. Carmele, J. Kabuss, F. Schulze, S. Reitzenstein, and A. Knorr, Single Photon Delayed Feedback: A Way to Stabilize Intrinsic Quantum Cavity Electrodynamics, *Physical Review Letters* **110**, 013601 (2013).

[21] N. L. Naumann, L. Droenner, S. M. Hein, A. Carmele, A. Knorr, and J. Kabuss, Feedback control of optomechanical systems, in *Physics and Simulation of Optoelectronic Devices XXIV*, Vol. 9742 (International Society for Optics and Photonics, 2016) p. 974216.

[22] Y. Lu, N. L. Naumann, J. Cerrillo, Q. Zhao, A. Knorr, and A. Carmele, Intensified antibunching via feedback-induced quantum interference, *Physical Review A* **95**, 063840 (2017).

[23] H. Pichler, S. Choi, P. Zoller, and M. D. Lukin, Universal photonic quantum computation via time-delayed feedback, *Proceedings of the National Academy of Sciences* **114**, 11362 (2017).

[24] H. M. Wiseman and G. J. Milburn, *Quantum Measurement and Control* (Cambridge University Press, Oxford, 2002) p. 231.

[25] M. H. Muñoz Arias, I. H. Deutsch, P. S. Jessen, and P. M. Poggi, Simulation of complex dynamics of mean-field p -spin models using measurement-based quantum feedback control, *Physical Review A* **102**, 022610 (2020).

[26] T. Grigoletto and F. Ticozzi, Stabilization Via Feedback Switching for Quantum Stochastic Dynamics, *IEEE Control Systems Letters* **6**, 235 (2021).

[27] D. R. Hjelme, A. R. Mickelson, and R. G. Beausoleil, Semiconductor laser stabilization by external optical feedback, *IEEE Journal of Quantum Electronics* **27**, 352 (1991).

[28] G. F. Franklin, J. D. Powell, and A. Emami-Naeini, *Feedback Control of Dynamic Systems* (Pearson, 2014).

[29] A. Kubanek, M. Koch, C. Sames, A. Ourjoumtsev, P. W. H. Pinkse, K. Murr, and G. Rempe, Photon-by-photon feedback control of a single-atom trajectory, *Nature* **462**, 898 (2009).

[30] G. G. Gillett, R. B. Dalton, B. P. Lanyon, M. P. Almeida, M. Barbieri, G. J. Pryde, J. L. O'Brien, K. J. Resch, S. D. Bartlett, and A. G. White, Experimental feedback control of quantum systems using weak measurements, *Phys. Rev. Lett.* **104**, 080503 (2010).

[31] M. Rafiee, A. Nourmandipour, and S. Mancini, Enforcing dissipative entanglement by feedback, *Physics Letters A* **384**, 126748 (2020).

[32] Z. Tan, P. A. Camati, G. C. Cauquil, A. Auffèves, and I. Dotsenko, Alternative experimental ways to access entropy production, *Phys. Rev. Research* **3**, 043076 (2021).

[33] A. Di Giovanni, M. Brunelli, and M. G. Genoni, Unconditional mechanical squeezing via backaction-avoiding measurements and nonoptimal feedback control, *Physical Review A* **103**, 022614 (2021).

[34] K. Koshino and Y. Nakamura, Control of the radiative level shift and linewidth of a superconducting artificial atom through a variable boundary condition, *New Journal of Physics* **14**, 043005 (2012).

[35] I.-C. Hoi, A. F. Kockum, L. Tornberg, A. Pourkabirian, G. Johansson, P. Delsing, and C. M. Wilson, Probing the quantum vacuum with an artificial atom in front of a mirror, *Nature Physics* **11**, 1045 (2015).

[36] A. L. Grimsmo, Time-Delayed Quantum Feedback Control, *Physical Review Letters* **115**, 060402 (2015).

[37] J. Kabuss, F. Katsch, A. Knorr, and A. Carmele, Unraveling coherent quantum feedback for Pyragas control, *Journal of the Optical Society of America B* **33**, C10 (2016).

[38] H. Pichler and P. Zoller, Photonic Circuits with Time Delays and Quantum Feedback, *Physical Review Letters* **116**, 093601 (2016).

[39] N. Német and S. Parkins, Enhanced optical squeezing from a degenerate parametric amplifier via time-delayed coherent feedback, *Physical Review A* **94**, 023809 (2016).

[40] S. M. Hein, A. Carmele, and A. Knorr, Creation and control of entanglement by time-delayed quantum-coherent feedback, in *Physics and Simulation of Optoelectronic Devices XXIV*, Vol. 9742 (International Society for Optics and Photonics, 2016) p. 97420X.

[41] P.-O. Guimond, H. Pichler, A. Rauschenbeutel, and P. Zoller, Chiral quantum optics with V-level atoms and coherent quantum feedback, *Physical Review A* **94**, 033829 (2016).

[42] S. J. Whalen, A. L. Grimsmo, and H. J. Carmichael, Open quantum systems with delayed coherent feedback, *Quantum Science and Technology* **2**, 044008 (2017).

[43] N. L. Naumann, S. M. Hein, M. Kraft, A. Knorr, and A. Carmele, Feedback control of photon statistics, in *Physics and Simulation of Optoelectronic Devices XXV*, Vol. 10098 (International Society for Optics and Photonics, 2017) p. 100980N.

[44] P.-O. Guimond, M. Pletyukhov, H. Pichler, and P. Zoller, Delayed coherent quantum feedback from a scattering theory and a matrix product state perspective, *Quantum Science and Technology* **2**, 044012 (2017).

[45] P. Forn-Díaz, C. Warren, C. Chang, A. Vadiraj, and C. Wilson, On-Demand Microwave Generator of Shaped Single Photons, *Physical Review Applied* **8**, 054015 (2017).

[46] S. J. Whalen, Collision model for non-Markovian quantum trajectories, *Physical Review A* **100**, 052113 (2019).

[47] N. Német, S. Parkins, A. Knorr, and A. Carmele, Stabilizing quantum coherence against pure dephasing in the presence of time-delayed coherent feedback at finite temperature, *Physical Review A* **99**, 053809 (2019).

[48] G. Calajó, Y.-L. L. Fang, H. U. Baranger, and F. Ciccarello, Exciting a Bound State in the Continuum through Multiphoton Scattering Plus Delayed Quantum Feedback, *Physical Review Letters* **122**, 073601 (2019).

[49] G. Crowder, H. Carmichael, and S. Hughes, Quantum trajectory theory of few-photon cavity-QED systems with a time-delayed coherent feedback, *Physical Review A* **101**, 023807 (2020).

[50] A. Harwood, M. Brunelli, and A. Serafini, Cavity optomechanics assisted by optical coherent feedback, *Physical Review A* **103**, 023509 (2021).

[51] K. Barkemeyer, M. Hohn, S. Reitzenstein, and A. Carmele, Boosting energy-time entanglement using coherent time-delayed feedback, *Physical Review A* **103**, 062423 (2021).

[52] Y. Shi and E. Waks, Deterministic generation of multidimensional photonic cluster states using time-delay feedback, *Physical Review A* **104**, 013703 (2021).

[53] S. Arranz Regidor, G. Crowder, H. Carmichael, and S. Hughes, Modeling quantum light-matter interactions in waveguide QED with retardation, nonlinear interactions, and a time-delayed feedback: Matrix product states versus a space-discretized waveguide model, *Physical Review Research* **3**, 023030 (2021).

[54] K. Barkemeyer, A. Knorr, and A. Carmele, Heisenberg treatment of multiphoton pulses in waveguide QED with time-delayed feedback, *Physical Review A* **106**, 023708 (2022).

[55] G. Crowder, L. Ramunno, and S. Hughes, Quantum trajectory theory and simulations of nonlinear spectra and multiphoton effects in waveguide-QED systems with a time-delayed coherent feedback, *Physical Review A* **106**, 013714 (2022).

[56] D. Istrati, Y. Pilnyak, J. C. Loredo, C. Antón, N. Somaschi, P. Hilaire, H. Ollivier, M. Esmann, L. Cohen, L. Vidro, C. Millet, A. Lemaître, I. Sagnes, A. Harouri, L. Lanco, P. Senellart, and H. S. Eisenberg, Sequential generation of linear cluster states from a single photon emitter, *Nature Communications* **11**, 5501 (2020).

[57] P. Steindl, H. Snijders, G. Westra, E. Hissink, K. Iakovlev, S. Polla, J. Frey, J. Norman, A. Gossard, J. Bowers, D. Bouwmeester, and W. Löfller, Artificial Coherent States of Light by Multiphoton Interference in a Single-Photon Stream, *Physical Review Letters* **126**, 143601 (2021).

[58] J.-P. Li, J. Qin, A. Chen, Z.-C. Duan, Y. Yu, Y. Huo, S. Höfling, C.-Y. Lu, K. Chen, and J.-W. Pan, Multiphoton Graph States from a Solid-State Single-Photon Source, *ACS Photonics* **7**, 1603 (2020).

[59] M. Cosacchi, T. Seidelmann, M. Cygorek, A. Vagov, D. Reiter, and V. Axt, Accuracy of the Quantum Regression Theorem for Photon Emission from a Quantum Dot, *Physical Review Letters* **127**, 100402 (2021).

[60] M. Richter and S. Hughes, Enhanced TEMPO Algorithm for Quantum Path Integrals with Off-Diagonal System-Bath Coupling: Applications to Photonic Quantum Networks, *Physical Review Letters* **128**, 167403 (2022).

[61] C. Gardiner and P. Zoller, *Quantum Noise: A Handbook of Markovian and Non-Markovian Quantum Stochastic Methods with Applications to Quantum Optics* (Springer-Verlag, Berlin, 2000).

[62] P. Stenius and A. Imamoglu, Stochastic wavefunction methods beyond the Born - Markov and rotating-wave approximations, *Quantum and Semiclassical Optics: Journal of the European Optical Society Part B* **8**, 283 (1996).

[63] D. Chruciński and A. Kossakowski, Non-Markovian Quantum Dynamics: Local versus Nonlocal, *Physical Review Letters* **104**, 070406 (2010).

[64] L. Tian and H. J. Carmichael, Quantum trajectory simulations of two-state behavior in an optical cavity containing one atom, *Physical Review A* **46**, R6801 (1992).

[65] J. Dalibard, Y. Castin, and K. Mølmer, Wave-function approach to dissipative processes in quantum optics, *Physical Review Letters* **68**, 580 (1992).

[66] M. N. Makhonin, J. E. Dixon, R. J. Coles, B. Royall, I. J. Luxmoore, E. Clarke, M. Hugues, M. S. Skolnick, and A. M. Fox, Waveguide Coupled Resonance Fluorescence from On-Chip Quantum Emitter, *Nano Letters* **14**, 6997 (2014).

[67] R. Uppu, F. T. Pedersen, Y. Wang, C. T. Olesen, C. Papon, X. Zhou, L. Midolo, S. Scholz, A. D. Wieck, A. Ludwig, and P. Lodahl, Scalable integrated single-photon source, *Science Advances* **6**, eabc8268 (2020).

[68] L. Dusanowski, C. Gustin, S. Hughes, C. Schneider, and S. Höfling, All-Optical Tuning of Indistinguishable Single Photons Generated in Three-Level Quantum Systems, *Nano Letters* **22**, 3562 (2022).

[69] See Supplemental Material at [URL will be inserted by publisher](#) for a discussion on the B_n operators and a comparison of Markovian and non-Markovian feedback.

- [70] R. H. Brown and R. Q. Twiss, Correlation between Photons in two Coherent Beams of Light, *Nature* **177**, 27 (1956).
- [71] C. K. Hong, Z. Y. Ou, and L. Mandel, Measurement of subpicosecond time intervals between two photons by interference, *Physical Review Letters* **59**, 2044 (1987).
- [72] P. Schnauber, A. Singh, J. Schall, S. I. Park, J. D. Song, S. Rodt, K. Srinivasan, S. Reitzenstein, and M. Davanco, Indistinguishable Photons from Deterministically Integrated Single Quantum Dots in Heterogeneous GaAs/Si3N4 Quantum Photonic Circuits, *Nano Letters* **19**, 7164 (2019).
- [73] C. Gustin, R. Manson, and S. Hughes, Spectral asymmetries in the resonance fluorescence of two-level systems under pulsed excitation, *Optics Letters* **43**, 779 (2018).
- [74] K. Mnaymneh, D. Dalacu, J. McKee, J. Lapointe, S. Hafouz, J. F. Weber, D. B. Northeast, P. J. Poole, G. C. Aers, and R. L. Williams, On-chip integration of single photon sources via evanescent coupling of tapered nanowires to SiN waveguides, *Advanced Quantum Technologies* **3**, 1900021 (2019).